

Dielectric properties of SrBi₂Ta₂O₉ films in the low-temperature range

PINGXIONG YANG*, MING GUO, MEIRONG SHI

College of Information Science and Technology, East China Normal University, 3663 Zhongshan North Road, Shanghai 200062, P. R. China

E-mail: pxyang@ee.ecnu.edu.cn

Published online: 1 November 2005

Ferroelectric materials, which show various interesting properties, such as high-dielectric constants, large spontaneous polarization, and optical nonlinearities, have attracted great attention for device application in nonvolatile memory, uncooled infrared detectors, and optical sensor protection [1–3]. In recent years, ferroelectric thin films are being used to develop a new class of tunable microwave devices. These devices are based on the large electric field dependent dielectric constant observed in ferroelectric materials, which are desirable to have a large capacitance change ratio [tunability(η) = $(C_{\max} - C_{\min})/C_{\max}$] under a certain electric-field range accompanied by a small dielectric loss. The devices employing ferroelectric films have high-tuning speed, high-radiation resistance, low power consumption, and low cost [4–9].

In this letter, we report on the dielectric properties and the voltage tunability of SrBi₂Ta₂O₉ thin films in low temperature range of 10–300 K. Origin for the temperature effect of the dielectric properties and the voltage tunability of SBT films, which may arise from switchable polarization that is frozen at lower temperature, is discussed. These results provide additional insight into their use for ferroelectric microwave device applications.

The SBT thin films were fabricated on platinized silicon (Pt/Ti/SiO₂/Si) using pulsed laser deposition (PLD) assisted by a dc glow discharge plasma. The laser used for SBT thin film deposition was an ArF (Lambda Physik LPX220icc, wavelength 193 nm) excimer laser with 5 Hz repetition frequency, 17 ns pulse duration, and an energy of 160 mJ/pulse. The output laser beam was focused onto a rotating SBT ceramic target at an angle of 45° by a UV lens with a focal length of 50 cm. The platinized silicon (Pt/Ti/SiO₂/Si) substrates were mounted onto a heated substrate holder and placed parallel to the target at a distance of 4–5 cm. The stability of the incoming beam was monitored using an energy meter. In order to minimize the chemical reaction between the film and substrate and control stoichiometry and structure, a low oxygen pressure dc glow discharge was used during laser deposition. A copper ring was placed halfway between the target and substrate. The substrate and target were electrically grounded while the ring was held at +700 V.

Before deposition, the chamber was initially pumped down to 5 Pa by a mechanical pump, and high purity oxygen was then introduced using a mass flow controller at a flow rate of 20 cm³/min, until an approximate pressure of 20 Pa was obtained. The films were deposited on the platinized silicon substrates at 400 °C during deposition, and annealed at 750 °C for 90 min in oxygen. Pt electrodes of 30 nm thickness and about 1.39 × 10⁻⁴ cm² area were deposited on the top surface of the films at 25 °C through a shadow mask using a UHV electron beam evaporator (Balzers UMS 500p) to complete the sandwich structure Pt/SBT/Pt film capacitor device. Compositional analysis was performed using inductively coupled plasma quantemeter and showed the ratio of Sr:Bi:Ta to be 1.0:1.98:2.0 for the SBT film.

The crystallographic structure of the SBT films was characterized by X-ray diffraction (XRD) using Cu K α radiation. The microstructure of the films was observed by atomic force microscopy (AFM). The ferroelectric behavior was investigated using an RT66A (Radiant Technologies). The dielectric properties and the voltage tunability of thin films were measured by a HP4194A Impedance/Gain-Phase Analyzer in the temperature range of 10–300 K at 100 kHz. These measured values were simulated by an equivalent circuit using an ideal capacitor shunted with an ideal resistor.

The crystallographic structure of SBT films was characterized by X-ray diffraction (XRD) using Cu K α radiation and the results are shown in Fig. 1. The XRD pattern shows that the dominant orientations of the films on platinized silicon are (008), (200), and (115). Compared with our previous work without the dc glow discharge assist [10], the films have an additional strong (008). This is due to the discharge plasma and the electrical poling of the 700 V bias field. During film growth using laser ablation, the role of the discharge plasma can be imagined in terms of modifying the growth kinetics. A dc discharge produces a flux of predominately O₂⁺, and O⁺ ions. In this experiment, the substrate was grounded electrically; O₂⁺, and O⁺ ions arrive at the substrate surface and react with the incumbent Bi atoms, increasing the probability of Bi incorporation into the film. Similarly, the grounding target electrically had limited Bi deviation at the target surface effectively [11]. Thus, as the Bi-deficient

* Author to whom all correspondence should be addressed.

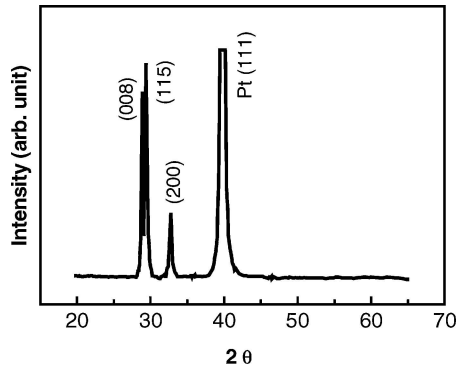


Figure 1 X-ray diffraction pattern of SBT films on platinized silicon (Pt/Ti/SiO₂/Si) substrates using pulsed laser deposition with dc glow discharge plasma.

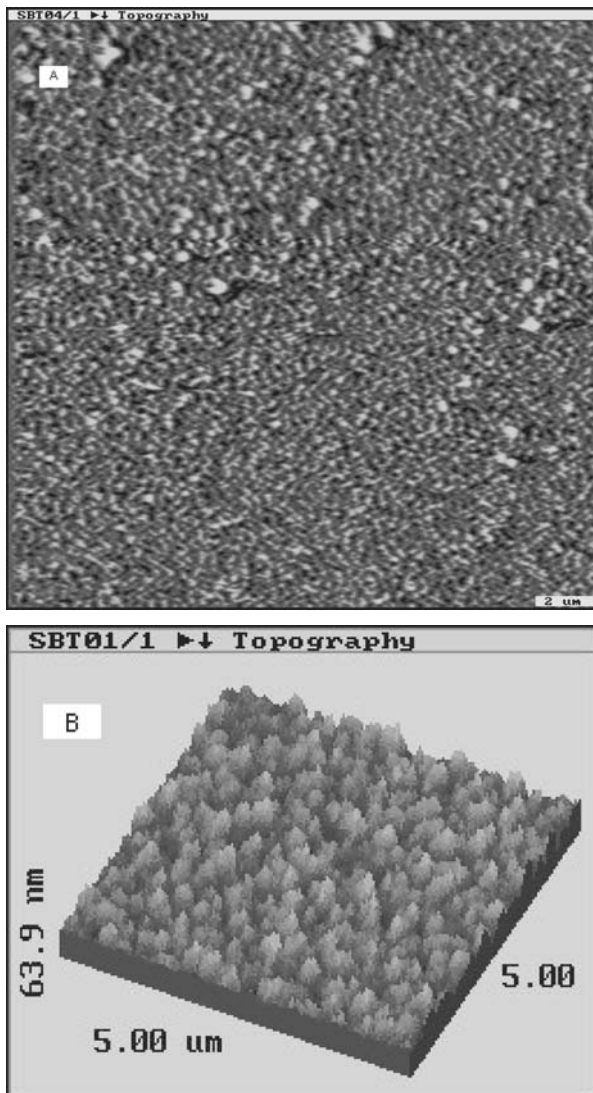


Figure 2 (a) The AFM images of SBT films's surface morphology and (b) three-dimensional topography.

pyrochlore phase [12] was reduced, the quality of the films was improved.

The AFM images of the films's surface morphology are displayed in Fig. 2. The surface of films is smooth, and the morphology displays a homogeneous crack-free appearance in all scanned areas of the sample in Fig. 2a. The observed microstructure is very dense. This may be the result of modifying the growth

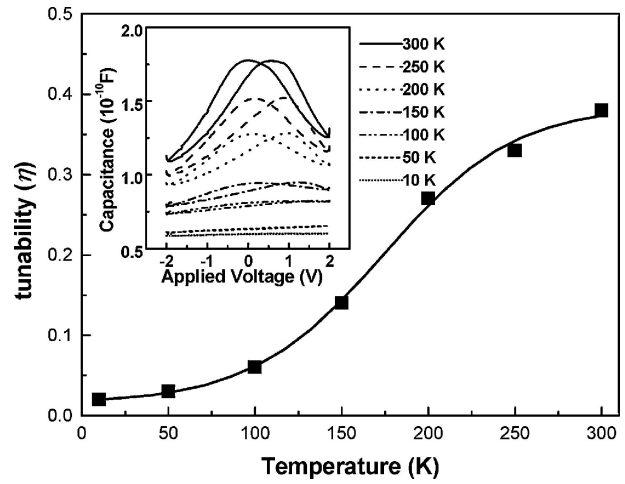


Figure 3 The temperature dependence for tunability of SBT films. The inset shows measured capacitance vs. voltage relations in the films as a function of temperature.

kinetics by the discharge plasma. The large average kinetic energy of the depositing species inherent in pulsed laser deposition and high-density target also likely contribute to the dense microstructure. The surface shows a mean grain size of about 300 nm. Moreover, the SBT film exhibits a columnar structure in Fig. 2b of three-dimensional topography, indicating that the grain growth process is dictated by nucleation at the substrate surface, as observed previously for SBT films by transmission electron microscopy [10]. This is an expected result for films prepared by physical vapor deposition processes.

Dielectric nonlinearity of the SBT films was examined by C–V measurement. Fig. 3 shows the tunability [$\eta = (C_{\max} - C_{\min}) / C_{\max}$] as a function of the temperature from 10 to 300 K. When the temperature is low, the tunability is low. On the other hand, the tunability decreased by decreasing the temperature. The tunability reached 38% at 300 K. This value is lower than that of BST [7, 8]. But the dielectric loss is about 0.0077, which is extremely low. Tunability/loss is about 49.4, which is larger than that reported for BST films [7, 8]. The dielectric nonlinearity as a function of the temperature from 10 to 300 K is clearly shown in the inset of Fig. 3. The C–V curves in the inset show maxima in the capacitance values at approximately the coercive field ($E_c = V_c/L$). The magnitudes of the maxima weaken with decreasing temperature, and essentially disappear at 10–100 K. As shown in the inset, the peaks with the direction of applied field scanning are asymmetric, which originates from the asymmetric conduction of the capacitor [13].

We assume that the capacitance consists of linear and nonlinear parts [14, 15]: $C = C_f + (dP(E)/dE)S/L$, where C_f is the linear capacitance, $P(E)$ is the polarization, E is the applied field, L is the thickness, and S is the area of the capacitor. From the equation above, the capacitance peaks in the inset of Fig. 3 correspond to polarization reversal, and the peak intensity depends on the amount of switchable polarization. With decreasing temperature, the amount of switchable polarization lessens due to domain pinning, or the freezing of domains, which suppresses the magnitude of peaks.

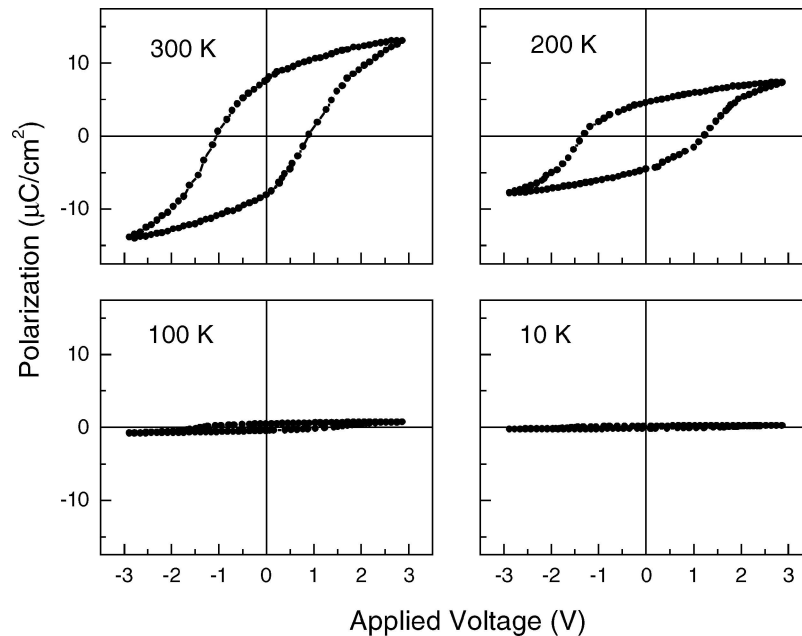


Figure 4 The polarization vs. applied voltage as a function of temperature.

Because of this, polarization reversal in the films is diminished resulting in the disappearance of the peaks in the capacitance, as illustrated in the inset of Fig. 3. Based on these arguments, we believe that the origin for the temperature effect of tunability may arise from switchable polarization that is frozen at lower temperature. Thus, the tunability decreased by decreasing the temperature in Fig. 3 due to domain pinning, or the freezing of domains, which suppresses the magnitude of capacitance peaks.

Further, the ferroelectric properties for SBT thin film were also measured by RT66A (Radiant Technologies) at low temperature. The polarization vs. applied voltage as a function of temperature was presented in Fig. 4. With decreasing temperature, the coercive field ($E_c = V_c/L$) is increasing, but the hysteresis loop become smaller and smaller, and the remanent polarization, resulting from the amount of switchable polarization, lessens due to domain pinning, or the freezing of domains at lower temperature, as illustrated in Fig. 4. The results of the ferroelectric measurements are in good agreement with dielectric constant measurements.

In summary, high-quality SBT/Pt heterostructures were fabricated for potential application in electrically tunable devices. The temperature dependence for tunability of SBT thin films with platinum electrodes (Pt/SBT/Pt) on silicon wafers was investigated from 10 to 300 K. Tunability/loss is about 49.4 at 300 K, which is larger than that reported for BST films. With decreasing temperature, the tunability decreased. The origin for the temperature effect of tunability is discussed. This effect may arise from switchable polarization that is frozen at lower temperature, which suppresses the magnitude of capacitance peaks. These results show SBT films to be promising materials for application in electrically tunable microwave devices, and are also necessary to fully characterize SBT for device applications in which a broader temperature range is anticipated.

Acknowledgment

This work was supported by Shanghai-Applied Materials Research and Development Fund, No. 0411.

References

1. J. F. SCOTT and C. A. ARAUJO, *Science* **246** (1989) 1400.
2. P. YANG, D. L. CARROLL and J. BALLATO, *J. Mater. Sci. Lett.* **22** (2003) 5.
3. P. YANG, J. XU, J. BALLATO, R. SCHWARTZ and D. CARROLL, *Appl. Phys. Lett.* **80** (2002) 3394.
4. J. IM, O. AUCIELLO, P. K. BAUMANN, S. K. STREIFFER, D. Y. KAUFMAN and A. R. KRAUSS, *ibid.* **76** (2000) 625.
5. W. CHANG, J. S. HORWITZ, A. C. CARTER, J. M. POND, S. W. KIRCHOEFER, C. M. GILMORE and D. B. CHRISSEY, *ibid.* **74** (1999) 1033.
6. S. HYUN and K. CHAR, *ibid.* **79** (2001) 254.
7. B. H. PARK, Y. GIM, Y. FAN, Q. X. JIA and P. LU, *ibid.* **77** (2000) 2587.
8. A. VOROBIEV, P. RUNDQVIST, K. KHAMCHANE and S. GEVORGIAN, *ibid.* **83** (2003) 3144.
9. M. W. COLE, W. D. NOTHWANG, C. HUBBARD, E. NGO and M. ERVIN, *J. Appl. Phys.* **93** (2003) 9218.
10. P. YANG, N. ZHOU, L. ZHENG, H. LU and C. LIN, *J. Phys. D: Appl. Phys.* **30** (1997) 527.
11. P. YANG, D. L. CARROLL, J. BALLATO and R. W. SCHWARTZ, *J. Appl. Phys.* **93** (2003) 9226.
12. M. A. RODRIGUEZ, T. J. BOYLE, B. A. HERNANDEZ, C. D. BUCHHEIT and M. O. EATOUGH, *J. Mater. Res.* **11** (1996) 2282.
13. L. ZHENG, C. LIN, W. XU and M. OKUYAMA, *J. Appl. Phys.* **79** (1996) 8634.
14. S. L. MILLER, R. D. NASBY, J. R. SCHWANK, M. S. RODGERS and P. V. DRESSENDORFER, *ibid.* **68** (1990) 6463.
15. S. L. MILLER, J. R. SCHWANK, R. D. NASBY and M. S. RODGERS, *ibid.* **70** (1991) 2849.

Received 1 September 2004
and accepted 22 July 2005